Clinical Imaging 55 (2019) 132–139

Contents lists available at ScienceDirect

Clinical Imaging

journal homepage: www.elsevier.com/locate/clinimag

Body Imaging

Usefulness of non-contrast MR imaging in distinguishing pancreatic ductal adenocarcinoma from focal pancreatitis

Jeong Hyun Lee[a], Ji Hye Min[b], Young Kon Kim[a,*], Dong Ik Cha[a], Jisun Lee[c], Hyun Jeong Park[d], Soohyun Ahn[e]

[a] Department of Radiology and Center for Imaging Science, Samsung Medical Center, Sungkyunkwan University School of Medicine, Seoul, Republic of Korea
[b] Department of Radiology, Chungnam National University Hospital, Chungnam National University College of Medicine, Daejeon, Republic of Korea
[c] Department of Radiology, Chungbuk National University Hospital, Cheongju, Republic of Korea
[d] Department of Radiology, Chung-Ang University Hospital, Chung-Ang University College of Medicine, Seoul, Republic of Korea
[e] Department of Mathematics, Ajou University, Suwon, Republic of Korea

ARTICLE INFO

Keywords:
Pancreatic ductal adenocarcinoma
Focal pancreatitis
MR imaging
MDCT
Gadoxetic acid

ABSTRACT

Background: Accurate differentiation between pancreatic adenocarcinoma and focal pancreatitis is challenging.
Purpose: To investigate the usefulness of non-contrast MRI by comparing with multidetector row CT (MDCT) and gadoxetic acid-enhanced MRI in the discrimination of pancreatic ductal adenocarcinoma (PDAC) and focal pancreatitis (FP).
Materials and methods: This retrospective study included 187 patients (116 with PDACs and 71 with FP) who underwent gadoxetic acid-MRI and MDCT prior to surgical resection or biopsy. The MRI features of PDAC and FP were compared by two radiologists. Then, two observers independently reviewed the three imaging sets: MDCT, non-contrast MRI (T1-, T2-weighted, and diffusion-weighted images), and MRI with and without gadoxetic acid to determine the diagnostic performances of each imaging modality in the discrimination of PDAC and FP.
Results: The significant features on non-contrast MRI for diagnosis of PDAC included peritumoral cyst, pancreatic duct cut-off, clear hypointensity on T1WI, and bile duct dilatation ($P < 0.05$). Presence of peritumoural cyst showed the highest odds ratio for predicting PDAC. Non-contrast MRI was superior to MDCT in differentiating PDAC from FP with regard to accuracy (84.5% vs 95.5% for observer 1; 85.8% vs. 96.0% for observer 2), sensitivity (83.6% vs. 98.3%; 84.5% vs 97.8%), and negative predictive value (76.3% vs. 97.0%; 77.6% vs 96.4%) ($P < 0.05$). We found similar diagnostic values between the non-contrast MRI and MRI with and without contrast ($P > 0.05$) for both observers.
Conclusion: Non-contrast MRI is better than MDCT and comparable to MRI with and without gadoxetic acid in differentiating PDAC from FP.

1. Introduction

Advances in imaging techniques and endoscopic biopsy have improved the capabilities for differentiating pancreatic neoplasms from “pseudotumors” which include various non-neoplastic space-occupying lesions [1,2]. As a result, unnecessary pancreatic resection that accompanies a relatively high morbidity rate has decreased [2,3]. Nevertheless, approximately 5–10% of pancreatectomies performed for suspected pancreatic ductal adenocarcinoma (PDAC) actually turn out to be pseudotumour on final pathologic examination [1,2]. Most of these solid pseudotumors represent inflammatory and/or benign conditions inducing fibrosis associated with chronic pancreatitis (henceforth collectively acknowledged as focal pancreatitis, or FP) [4].

Differentiating FP from PDAC is still challenging, and confirming the indolent natural course is frequently the most reliable way to accomplish this task while avoiding surgery. But, this can be judged only after several serial imaging and clinical follow-up sessions has passed, of which approach consequently may deprive early PDAC patients the opportunity of receiving curative resection while watching and waiting for the character of an initially indeterminate lesion to become obvious. Therefore, pre-operative differentiation between FP and PDAC remains as an unsolved topic demanding further investigation.

Computed tomography (CT) is currently the most widely used modality to evaluate patients with suspected pancreatic malignancy.

* Corresponding author at: Department of Radiology and Center for Imaging Science, Samsung Medical Center, Sungkyunkwan University School of Medicine, 50, Ilwon-Dong, Kangnam-Ku, Seoul 135-710, Republic of Korea.
E-mail address: youngkon0707.kim@samsung.com (Y.K. Kim).

https://doi.org/10.1016/j.clinimag.2019.02.013
Received 26 October 2018; Received in revised form 14 February 2019; Accepted 19 February 2019

Table 1
MRI sequences and parameters.

Sequence	TR/TE (msec)	FA	Section thickness	Matrix size	Bandwidth (Hz/pixel)	Field of view (cm)	Acquisition time (sec)	No. of excitations
T1W-3D dual GRE	3.5/1.15–2.3	10°	6 mm	256 × 194	434.4	32–38 cm	14	1
BH-MS-T2WI	1623/70	90°	5 mm	324 × 235	235.2	32–38 cm	55	1
RT-SSH-HT2WI	1156/160	90°	5 mm	320 × 256	317.9	32–38 cm	120	2
T1W-3D GRE	3.1/1.5	10°	2 mm	256 × 256	995.7	32–38 cm	16.6	1
DWI	1600/70	90°	5 mm	112 × 112	79.5	32–38 cm	126	2
BH-2D-MRCP	6417/920	90°	40 mm	256 × 256	438.2	25 cm	3	1
NT-3D-MRCP	1673/650	90°	2 mm	320 × 206	607.6	35 cm	180–240	2

GRE = gradient echo, BH-MS-T2WI = breath-hold multishot T2-weighted image, RT-SSH-T2WI = respiratory-triggered single-shot heavily T2-weighted image, DWI = diffusion-weighted imaging, BH-2D-MRCP = breath-hold two-dimensional single-projection MR cholangiopancreatography, NT-3D-MRCP = navigator-triggered three-dimensional MR cholangiopancreatography.

However, some PDACs present as isoattenuating lesions being obscured in the pancreatic parenchyma, and now and then become invisible on CT [5]. A number of recently published studies have recognized the value of magnetic resonance imaging (MRI) in differentiating between PDAC and FP [6–10]. The majority of these reports have focused on differentiating focal autoimmune pancreatitis (AIP) and PDAC using a standard MR protocol with and without contrast. Diffusion-weighted imaging (DWI) has also proven useful in the detection of small or isoattenuating PDACs [11,12]. Considering the further increasing role of MRI for PDAC assessment, safety issues raised by the administration of gadolinium contrast agent such as nephrogenic systemic fibrosis and gadolinium accumulation in the brain seem to deserve further emphasis [13]. The increasing financial cost burdened by the increasing number of MR studies is another issue that is not trivial. Therefore, it would be worthwhile to adopt a non-contrast MR protocol with quicker scanning capabilities to not only avoid gadolinium associated complications, but also shorten the study time and consequently reduce the cost of MRI. Given that unenhanced T1- and T2-weighted images (T1WI, T2WI, respectively) provide excellent contrast resolution and detailed morphologic anatomy of the pancreatic duct (p-duct), we hypothesized that the diagnostic performance of non-contrast pancreas MRI (T1WI, T2WI, and DWI) may be comparable to that of the MRI with and without contrast.

The purpose of this study was to assess the usefulness of non- contrast MRI (T1WI, T2WI, and DWI) in the differentiation of PDAC and FP by comparing it with multidetector row CT (MDCT) and MRI with and without contrast.

2. Material and methods

2.1. Study population

Our institutional review board approved this retrospective study, and the requirement for informed consent was waived. We searched our institution's radiology report database for MRI reports (created between October 2008 and May 2017) that contained terms such as “ductal adenocarcinoma,” “pancreatic cancer,” “mass-forming,” “autoimmune pancreatitis,” “IgG4,” and “focal pancreatitis.” This query yielded 1378 patients with histologically proven pancreatic malignancy and 328 patients without histologic evidence of pancreatic malignancy.

Among these patients, we identified 855 who had undergone both CT and MRI. Patients confirmed as PDAC by surgery were included in the PDAC group, however for analysis we excluded patients obvious imaging findings that indicated malignancy (such as vascular invasion). Inclusion criteria for the FP group were as follows: histologic evidence of FP presenting with a focal pancreatic lesion on imaging; no histologic evidence of malignancy; and disappearance of the lesion on follow-up imaging study (in unresected cases). All participants underwent both a preoperative (or preprocedural) CT and MRI exam within a two-week interval. Ultimately, 116 patients (65 men, 51 women; mean age ± SD [standard deviation], 53.1 ± 8.9 years) with PDAC and 71 patients (54 men, 17 women; mean age ± SD, 62.1 ± 10.4 years) with FP met the inclusion criteria.

2.2. MDCT and MR examination

Multiphasic CT was conducted using either a 40-MDCT scanner (Brilliance 40; Philips Healthcare, Best, The Netherlands) or a 64-MDCT scanner (Aquilion 64; Toshiba Medical, Tokyo, Japan and Light Speed VCT 64; GE Healthcare, Waukesha, WI, USA). The scanning parameters were 120 kVp, 189–200 mAs, 5-mm slice thickness with an increment (overlap) of 2.5 mm, table speed of 26.5–39.37 mm/rotation (pitch 0.828–1.07), and a single-breath-hold helical acquisition of 4–6 s, depending on liver size. Arterial phase (AP) and portal venous phase (PVP) scanning began 30–40s and 70s, respectively, after injection of 110 or 120 mL of the nonionic iodinated contrast agent iopamidol (Iopamiro 300, Bracco) at a rate of 3–4 mL/s. The contrast was administered using a bolus-triggered technique.

MRIs were acquired using a 3.0-T MRI system (InteraAchieva; Philips Healthcare, Best, The Netherlands) equipped with 32-channel phased-array receiver coil. For gadoxetic acid-enhanced imaging, unenhanced, AP (20–35 s), PVP (60 s), late-phase (3 min), and 20-min hepatobiliary phase image were obtained using a T1-weighted 3D turbo-field-echo sequence (T1 high-resolution isotropic volume examination [THRIVE; Philips Healthcare]). Contrast agent was administered using a power injector at a rate of 1 mL/s for a dose of 0.025 mmol/kg body weight, followed by 20-mL saline flush. Diffusion-weighted imaging (DWI) was obtained by respiratory-triggered single-shot echo with b-values of 0, 100, and 800 s/mm^2. The detailed parameters of the MR sequences are shown in Table 1.

2.3. Image analysis

Image analysis consisted of two sessions. Initially, MRI was evaluated independently by two abdominal radiologists (H. J. P. and Y.K.K., with 9 and 18 years of experience, respectively), who were blinded to the patient information. These radiologists interpreted MRI with regard to lesion location, size, and the following imaging features: (a) peritumoral cyst; (b) enhancement pattern, (c) duct cut-off sign, (d) signal intensity on T1-weighted images (T1WI), (e) bile duct dilatation, and (f) rim sign. Peritumoral cyst was characterized by small irregular-, oval-, or linear-shaped fluid signal intensity seen in the periphery of the mass or adjacent to the mass (Fig.1). The enhancement pattern was divided into two categories. Type 1 was characterized by low-low-low, and type 2 by low-low-iso or low-isoiso signal intensity compared to normal pancreas parenchyma on the AP, PVP, and 3-min delayed phases, respectively. If the main pancreatic duct was found dilated, then the presence or absence of either duct cut-off or tapering were marked. The degree of hypointensity on precontrast T1WI was categorized into one of the following three grades: grade 1: isointense to normal pancreas

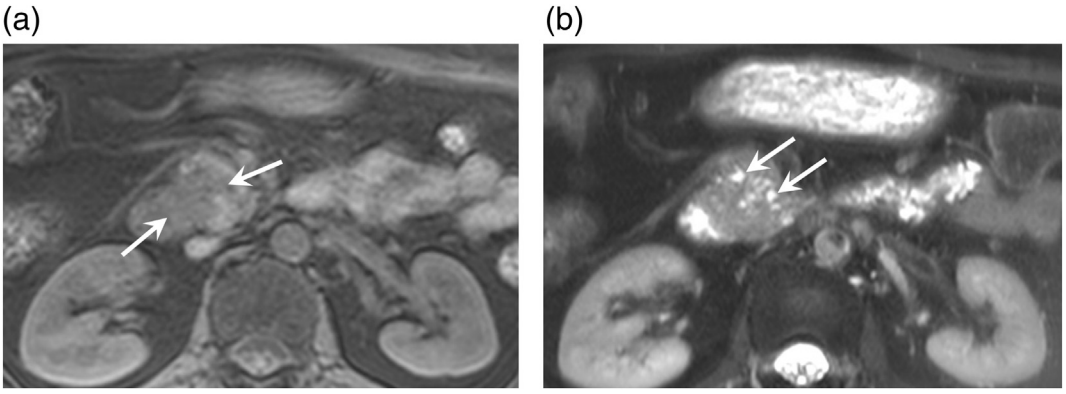

Fig. 1. Imaging patterns of pancreatic ductal adenocarcinoma that is seen as hypointense (arrow) lesion on unenhanced T1-weighted image (A), accompanying peritumoral cysts on T2-weighted image (arrows) (B).

parenchyma or spleen; grade 2: hypointense to the spleen but hyperintense to the renal medulla; and grade 3: hypointensity similar to that of the renal medulla [10]. The rim sign, indicating AIP, was defined by a rim of different signal intensity along the periphery of the lesion on T2WI or contrast-enhanced images [14]. The reviewers also determined the relative attenuation of PDAC on MDCT by grading the lesion in comparison to that of the adjacent normal pancreas as either hypoattenuation, isoattenuation (invisible) or hyperattenuation. After independently evaluating the images, the two observers reached a consensus for discordant findings.

In the second session, two off-site observers (J. H. M. and J. L. with 7 and 6 years of experience in pancreatic imaging, respectively), who were blinded to the patient information independently and separately analyzed the MDCT and non-contrast MRI sets within a four-week interval. Each observer was instructed to assign a score for each lesion using a 5-point scale (1, probably FP; 2, possibly FP; 3, indeterminate; 4, possibly PDAC; 5, probably PDAC). The criterion for PDAC was the presence of a discrete mass (hypoattenuating on MDCT or hypointense similar to the renal medulla on T1WI with hyperintensity on T2WI and DWI) with an abrupt cut-off of the dilated pancreatic duct distal to the mass. In contrast, criterion for FP was a poorly-defined, faintly delineated mass with or without smooth, tapered upstream p-duct dilatation. An invisible focal lesion with a p-duct cut-off was assigned as indeterminate. The presence of a peritumoral cyst had a high odds ratio of predicting PDAC in the results of the first review session. Therefore, when reviewing the non-contrast MRI set, the two observers were asked to score the lesions giving preference to the presence of a peritumoural cyst as favoring PDAC. The observers were also asked to review the MRI with and without contrast to determine whether the diagnosis on non-contrast MRI would be changed after adding gadoxetic acid-enhanced MRI.

2.4. Statistical analysis

For statistical analysis, lesions were divided into the following three groups: score 1–2, PDAC; score 3, indeterminate; score 4–5, FP. The sensitivity, specificity, accuracy, positive predictive value (PPV), and negative predictive value (NPV) for the diagnosis of PDAC were calculated according to the observer and modality used. Lesions with a score of 3 (indeterminate) were arbitrarily given a probability of 0.5 for calculation [15]. The differences in each parameter between the two imaging modalities were compared using Bennett's test or the McNemar test.

Interobserver reliability analysis was performed using Cohen's kappa statistics. The strength of the agreement was determined as follows: a kappa value < 0 indicates poor agreement; 0.000–0.200, slight; 0.201–0.400, fair; 0.401–0.600, moderate; 0.601–0.800, substantial; and 0.801–1.000, almost perfect agreement.

The frequency of specified MRI features in the PDAC group and FP group was calculated and compared using Fisher's exact test and Chi-square test.

All statistical analyses were performed using SAS version 9.4 (SAS Institute Inc., Cary, NC, USA) and R version 3.3.1 (Vienna, Austria). *P*-values < 0.05 were considered statistically significant (two-tailed).

3. Results

3.1. Patient demographics

The characteristics of the study patients and lesions are shown in Table 2. The diameter of the 116 PDACs ranged from 1.0 to 4.0 cm (mean ± SD, 2.57 ± 0.77 cm), and the diameter of the 71 FPs ranged from 1.0 to 5.1 cm (mean ± SD, 2.56 ± 0.95 cm). Both PDAC and FP were most commonly seen in pancreas heads (71.6% [83/116] vs. 60.6% [43/71]). All PDAC lesions were surgically confirmed. The histopathologic diagnosis of FP was confirmed with surgical specimens in 12 patients (16.9%), by open biopsy in 19 patients (26.8%), and by endoscopic ultrasound (EUS)-guided biopsy in 40 patients (56.3%). Twenty-five (35.2%) of the 71 FPs were a focal type of AIP, while the remaining 46 (64.8%) were chronic pancreatitis with or without acute pancreatitis.

Table 2
Demographic and pathological characteristics of 187 patients with pancreatic ductal adenocarcinoma or focal pancreatitis

Characteristics	PDAC (*N* = 116)	FP (*N* = 71)	p-Value
Age (y)[a]	63.4 ± 10.4 (31–85)	57.7 ± 10.5 (30–79)	0.045
Male/Female	65/51	54/17	0.006
Lesion size (cm)[a]	2.54 ± 0.79 (1.0–4.0)	2.56 ± 0.98 (1.0–5.1)	0.981
> 2 cm	73 (62.9)	47 (66.2)	
≤ 2 cm	43 (37.1)	24 (33.8)	
Location			0.248
Head	83 (71.6)	43 (60.6)	
Body	19 (16.4)	14 (19.7)	
Tail	14 (12.0)	14 (19.7)	
Pathology			–
Surgical resection	116 (100)	12 (16.9) [5 AIPs]	
Biopsy	–	59 (83.1)	

Note.—PDAC = pancreatic ductal adenocarcinoma; FP = focal pancreatitis; AIP = autoimmune pancreatitis.

[a] Data represent mean ± standard deviation, and data in parentheses represent range.

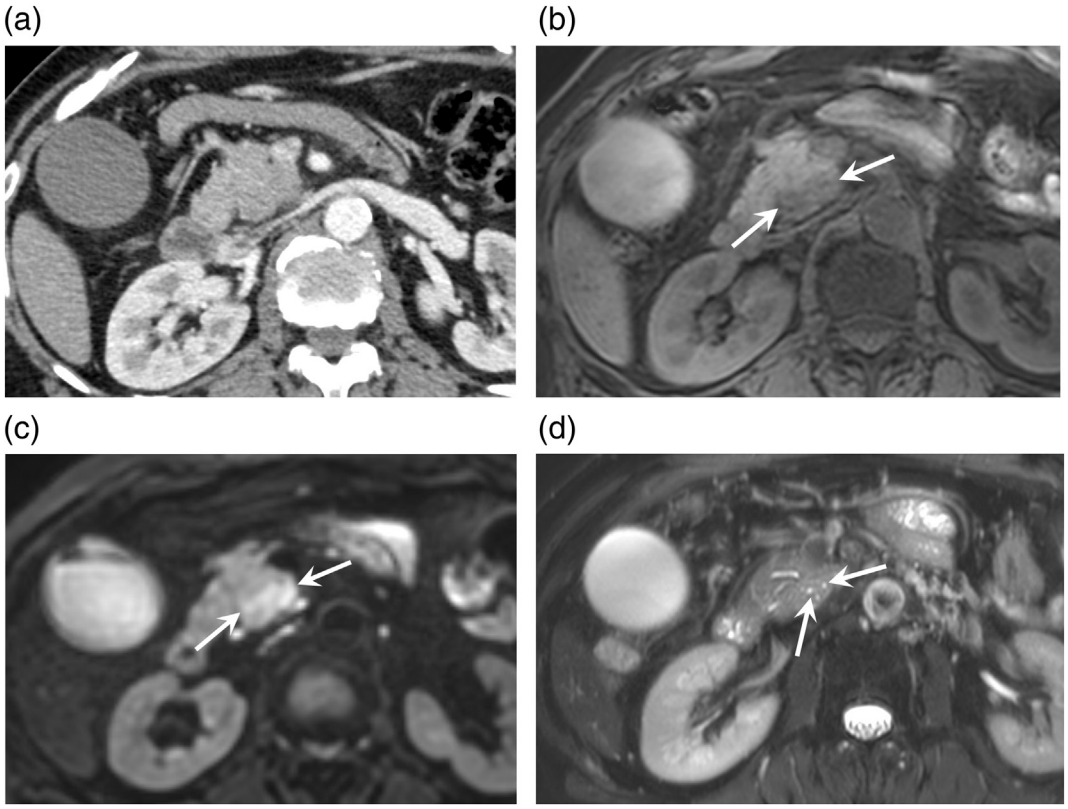

Fig. 2. Pancreatic ductal adenocarcinoma (2.6 cm in diameter) in a 70-year-old man. The pancreatic tumor is not clearly seen on the pancreatic phase image (A) or portal venous phase (not shown) of MDCT. The tumor (arrows) is clearly seen as hypointense on unenhanced T1-weighted MRI (B) and hyperintense on single-shot echo-planar DW imaging using $b = 800\ s/mm^2$(C). Tiny perilesional cysts (arrows) are seen as bright foci on the T2-weighted image (D) slightly lower level than (B) and (C), indicating malignancy.

3.2. MDCT and MRI features of PDAC and FP

On MDCT, 43 PDACs (75.9%) were depicted as hypoattenuating masses on either or both AP and PVP images. The remaining 28 (24.1%) were isoattenuating lesions with upstream p-duct dilatation (Fig. 2).

Table 3 summarizes the descriptive statistics of the MRI features. The PDAC group more frequently had the following features than did the FP group: peritumoral cyst (84.5% vs. 15.5%, $p < 0.0001$), type 1 enhancement pattern (60.3% vs. 18.3%, $p < 0.0001$), p-duct cut-off sign (68.1% vs. 18.4%, $p < 0.0001$), grade 3 hypointensity similar to the signal intensity of the renal medulla on T1WI (70.7% vs. 28.2%, $p < 0.0001$), and bile duct dilatation (68.1% vs. 47.9%, $p = 0.0061$). The rim sign was seen in focal AIP, but not in PDAC (0% vs. 11.3%, $p = 0.0003$). Peritumoral cyst had the highest odds ratio (28.85) to be associated with PDAC (Figs. 1,2), followed by p-duct cut-off (9.07), signal intensity on T1WI (6.08), bile duct dilatation (2.31), and the enhancement pattern (0.15). The interobserver agreement for all MRI findings was substantial to perfect (k = 0.61–0.86; k = 0.81 for peritumoral cyst, k = 0.61 for enhancement pattern, k = 0.75 for p-duct cut-off, k = 0.84 for signal intensity on T1WI, k = 0.85 for bile duct dilatation, and k = 0.86 for rim sign).

3.3. Diagnostic performance of MDCT and MRI

The distribution of lesions according to scores on MDCT and non-contrast MRI are presented in Table 4. The sensitivity, specificity, accuracy, PPV, and NPV for the diagnosis of PDAC by observer and modality are presented in Table 4. The overall diagnostic performance tended to be higher with non-contrast MRI or whole MRI than it was with MDCT for both observers. There were significant differences in sensitivity (83.6% vs. 98.3% for observer 1, $p = 0.0001$; 84.5% vs. 97.8% for observer 2, $p = 0.0002$), accuracy (84.5% vs. 95.5% for observer 1, $p = 0.0114$; 85.8% vs. 96.0% for observer 2, $p = 0.0197$), and NPV (76.3% vs. 97.0% for observer 1, $p = 0.0004$; 77.6% vs. 96.4% for observer 2, $p = 0.0007$). One misclassified PDAC and 32 indeterminate lesions on MDCT were accurately characterized by observer 1 with non-contrast MRI (Fig. 3). Meanwhile, two misclassified PDACs and 27 indeterminate lesions on MDCT were accurately characterized by observer 2 with non-contrast MRI. There were 10 and 12 FPs assigned as category 3 or 4 by each observer, respectively, but were correctly classified with non-contrast MRI (Fig.4).

We found similar diagnostic values between the non-contrast MRI and MRI with and without contrast ($P = 0.0.98–1.000$) for both observers. Adding gadoxetic acid-enhanced MRI to non-contrast MRI led to 1–2 additional correct diagnoses for each observer; two FPs assigned as category 3 on non-contrast MRI were correctly classified on the MRI with and without contrast by observer 1 and were assigned as category 3 and 2, respectively by observer 2 (Fig.5).

3.4. Interobserver agreement

Interobserver reliability analysis demonstrated almost perfect agreement in both MDCT and MRI scoring sessions (k = 0.876 for MDCT, k = 0.914 for non-contrast MRI; k = 0.901 for MRI with and without contrast; $p < 0.0001$, all).

4. Discussion

The primary goal of diagnostic imaging for PDAC is tumor detection, characterization, and differentiation from FP. Detection and characterization cannot be considered as separate processes, because missed PDACs are ultimately managed in the same way as benign

Table 3
MR imaging characteristics of patients with focal pancreatitis and pancreatic ductal adenocarcinoma.

MRI feature	PDAC (N = 116)	FP (N = 71)	Total (*N* = 187)	Odds ratio (95% CI)	p-Value[a]
Peritumoural cyst				28.85 (12.33–73.70)	< 0.0001
Absent	18 (15.5%)	60 (84.5%)	78 (41.7%)		
Present	98 (84.5%)	11 (15.5%)	109 (58.3%)		
Enhancement pattern				0.15 (0.07–0.31)	< 0.0001
Type 1	70 (60.3%)	13 (18.3%)	83 (44.4%)		
Type 2	46 (39.7%)	58 (81.7%)	104 (55.6%)		
Duct cut-off sign				9.07 (4.20–20.77)[†]	< 0.0001
No dilatation	4 (3.4%)	8 (11.3%)	12 (6.4%)		
Duct tapering	33 (28.4%)	50 (70.4%)	83 (44.4%)		
Duct cut-off	79 (68.1%)	13 (18.4%)	92 (49.2%)		
Signal intensity on T1WI				6.08 (3.05–12.51)[‡]	< 0.0001
Grade 1	18 (15.5%)	32 (45.1%)	50 (26.7%)		
Grade 2	16 (13.8%)	19 (26.8%)	35 (18.7%)		
Grade 3	82 (70.7%)	20(28.2%)	102 (54.6%)		
Bile duct dilatation				2.31 (1.21–4.46)	0.0061
Absent	37 (31.9%)	37 (52.1%)	74 (39.6%)		
Present	79 (68.1%)	34 (47.9%)	113 (60.4%)		
Rim sign				0 (0.00–0.33)	0.0003
Absent	116 (100%)	63 (88.7%)	179 (95.7%)		
Present	0 (0%)	8 (11.3%)	8 (4.3%)		

Note.—PDAC = pancreatic ductal adenocarcinoma; FP = focal pancreatitis; CI = confidence interval.
[a] Fisher's exact test.
[†] Odds ratio of duct cut-off, reference: duct tapering, $p < 0.0001$ (Fisher's exact test).
[‡] Odds ratio of grade 3, reference: grade 1 + grade 2, $p < 0.0001$ (Fisher's exact test).

lesions. In our study, we used stringent diagnostic criteria incorporating tumor delineation and secondary signs that are most predictive of PDAC. Therefore, cases that demonstrated abrupt p-duct cut-off without a clearly visible focal pancreatic lesion were considered as indeterminate lesions. The most clinically relevant diseases to be considered in this scenario would be visually isoattenuating PDAC and FP, including focal type of AIP [16].

Our study demonstrated that non-contrast MRI was superior to MDCT in the differentiation of PDAC from FP with regard to accuracy, sensitivity, and NPV. Another noteworthy finding is that non-contrast MRI showed almost the same diagnostic performance as MRI with and without contrast. Twenty-eight PDACs (24.1%) were isoattenuating on MDCT. Meanwhile, 98 PDACs showed some degree of hypointensity on T1WI (grade 2 and 3, 84.5%). Therefore, our results can be at least partially explained by the superiority of non-contrast MRI in tumor delineation compared to MDCT, in similar lines with a prior report which showed that 17 of 19 isoattenuating PDAC were hypointense on T1WI [16]. In the current study, addition of gadoxetic acid only led to an additional 1–2 correctly identified cases (FP) by each observer. Four PDACs in this study had no dilatation of either the p-duct or bile duct. These lesions all showed grade 3 hypointensity on T1WI, and three of them were correctly classified as PDAC by applying the peritumoral

Table 4
Diagnostic performance by observer and modality.

Score	Observer 1				Observer 2			
	MDCT	Non-contrast MRI	Whole MRI	p-Value …	MDCT	Non-contrast MRI	Whole MRI	p-Value …
1	18 [0/18]	25 [0/25]	32[0/32]		21 [0/21]	27 [0/27]	33[0/33]	
2	38 [2/36]	37 [1/36]	33[1/32]		37 [3/34]	39 [1/38]	34[1/33]	
3	48 [34/14]	9 [2/7]	7 [2/5]		45 [30/15]	5 [3/2]	6 [3/3]	
4	29 [26/3]	41 [38/3]	38 [36/2]		39 [38/1]	38 [34/4]	30 [28/2]	
5	54 [54/0]	75 [75/0]	77 [77/0]		45 [45/0]	78 [78/0]	84 [84/0]	
Sensitivity (%)	83.6 (80)	98.3 (113)	98.3 (113)	0.0001/1.000	84.5 (83)	97.8 (112)	97.8 (112)	0.0002/1.000
Specificity (%)	85.9 (54)	90.8 (61)	93.7 (63)	0.268/0.317	88.0 (55)	93.0 (65)	95.1 (66)	0.243/0.289
Accuracy (%)	84.5 (134)	95.5 (174)	96.5 (176)	0.011/0.144	85.8 (138)	96.0 (177)	96.8 (178)	0.019/0.098
PPV (%)	90.7 (3)	94.6 (3)	96.2 (2)	0.145/0.320	92.0 (1)	95.8 (4)	97.0 (2)	0.152/0.291
NPV (%)	76.3 (2)	97.0 (1)	97.1 (1)	0.0004/0.951	77.6 (3)	96.4 (1)	96.4 (1)	0.019/0.963

Note - Data are numbers in parentheses, correctly interpreted lesions for accuracy, true positives for sensitivity, true negatives for specificity, false positives for PPV, and false negatives for NPV. Numbers in brackets represent the number of PDAC and FP, respectively. PPV: positive predictive value; NPV: negative predictive value. *P* values are MDCT vs. non-contrast MRI/non-contrast MRI vs whole MRI.

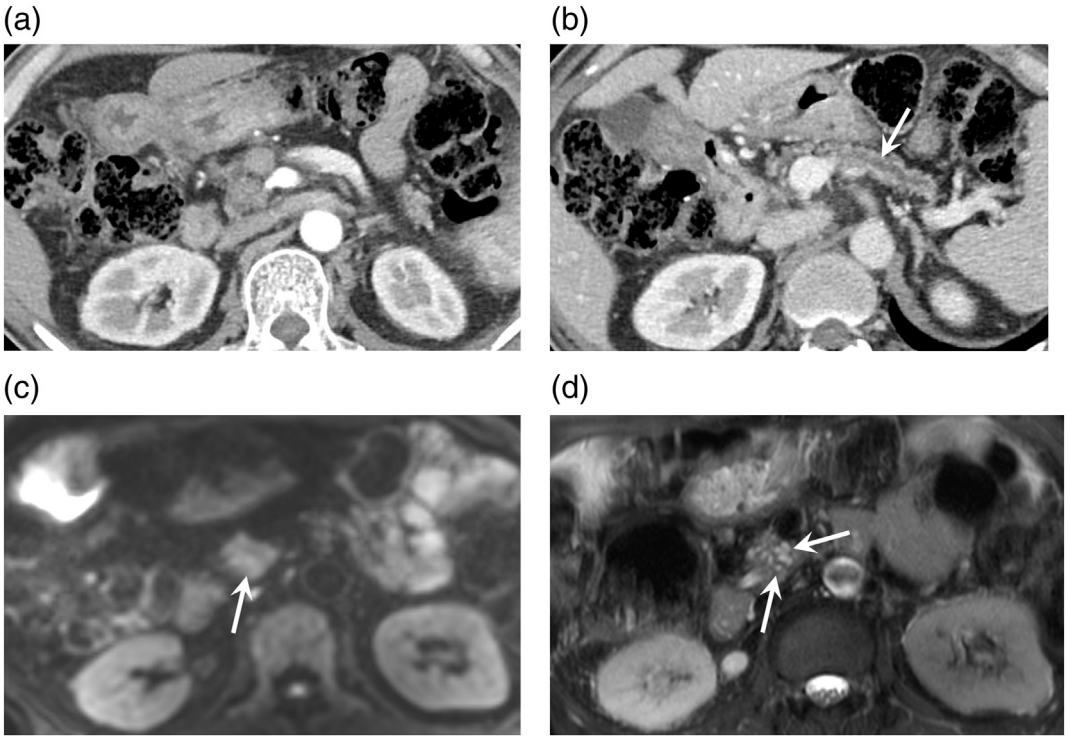

Fig. 3. Pancreatic ductal adenocarcinoma (1.7 cm in diameter) in a 66-year-old man. The pancreatic head mass is not clearly defined on the pancreatic phase image (A), but dilated distal pancreatic duct (arrow) is noted on the portal venous phase (B) of MDCT. The lesion was assigned as category 3 indeterminate lesion by both observers The tumor (arrow) is seen as hyperintense on single-shot echo-planar DW imaging using $b = 800\,s/mm^2$ (C). Multiple peritumoral cysts (arrows) are seen as bright foci on the T2-weighted image (D), indicating malignancy.

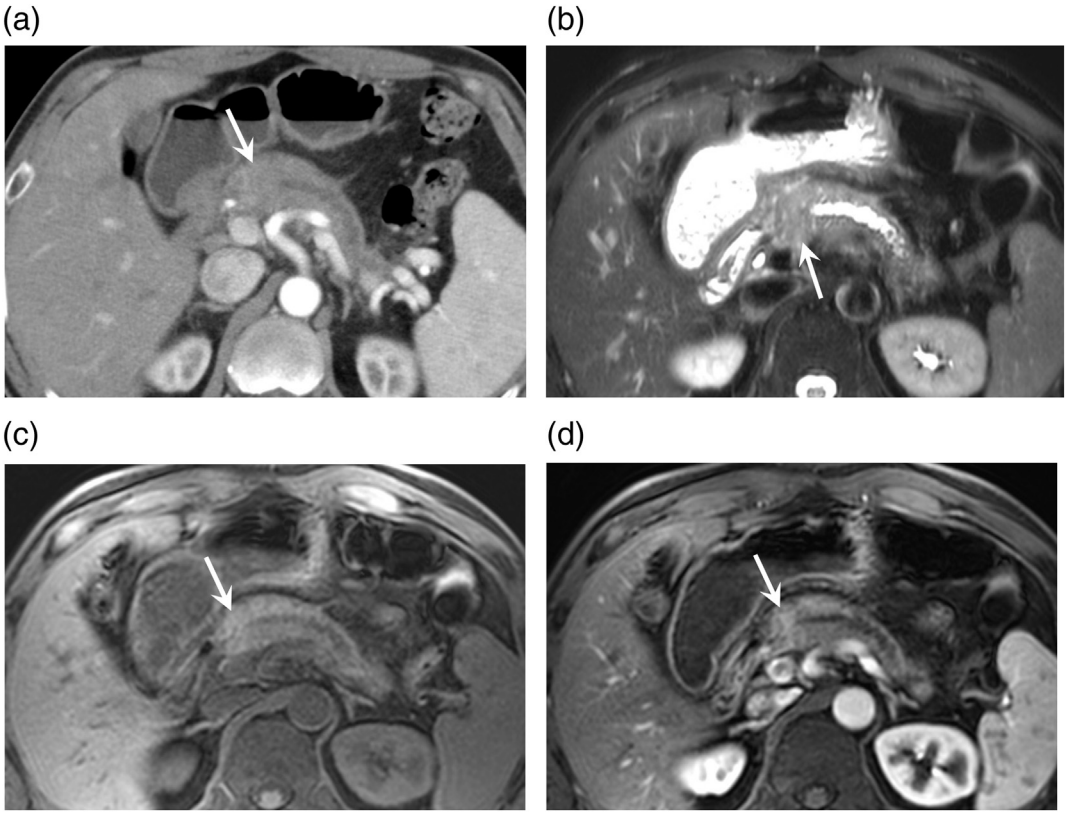

Fig. 4. Focal chronic pancreatitis (2.7 cm in diameter) in a 66-year-old man. The pancreatic mass (arrow) is seen as a subtle hypoattenuation proximal to obstructive pancreatic duct on the pancreatic phase image (A) of MDCT. The lesion was assigned as category 4 by each observer. The lesion (arrows) is not clearly delineated on T2-weighted image (B), unenhanced T1-weighted image (C), and on pancreatic phase after administration of gadoxetic acid (D).

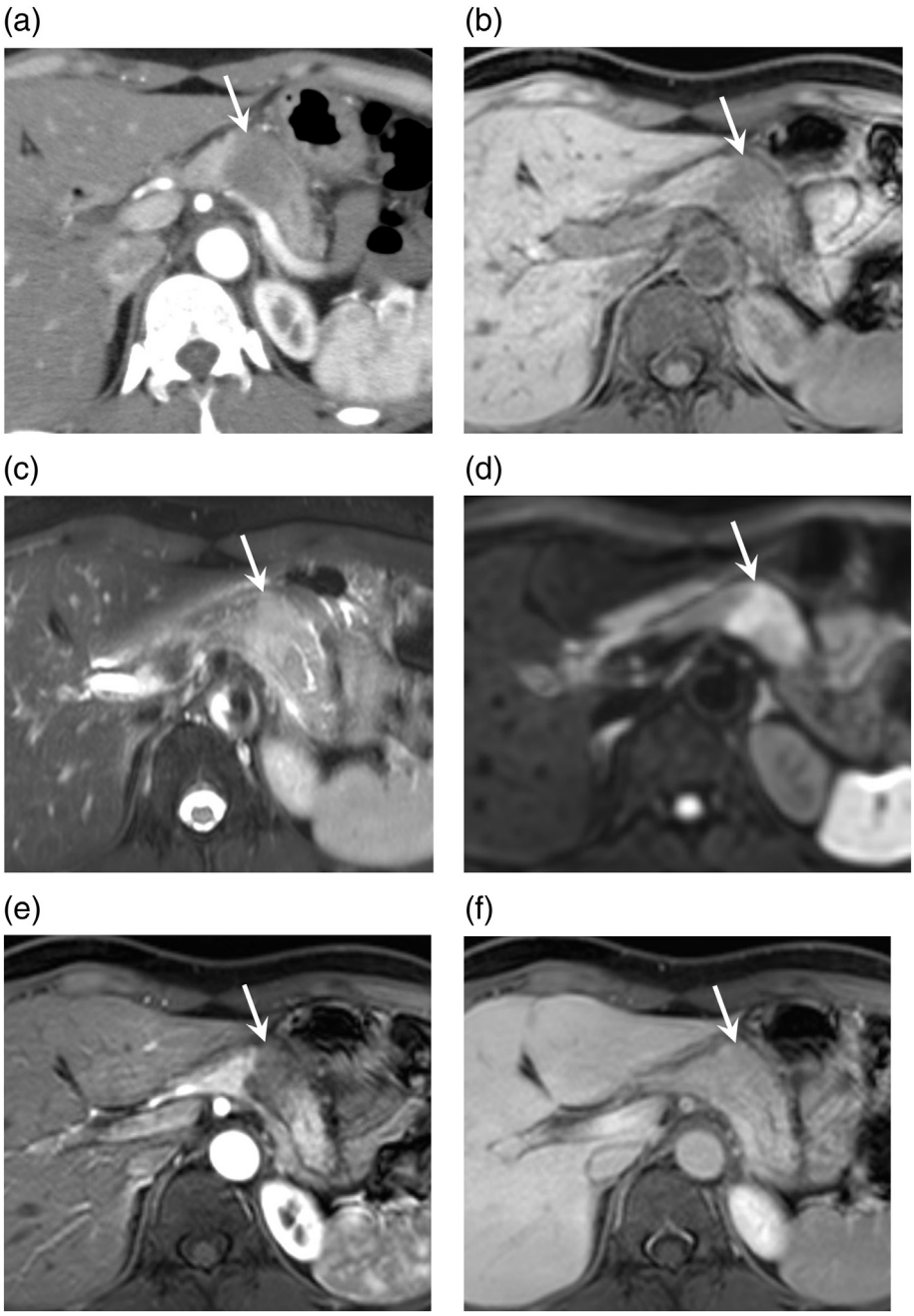

Fig. 5. Autoimmune pancreatitis (3.0 cm in diameter) in a 50-year-old woman. On the pancreatic phase image of MDCT (A), the pancreatic mass (arrow) is seen as a hypoattenuating lesion in the pancreas body and there is dilated obstructed pancreatic duct in the tail. The lesion (arrows) is clearly hypointense on unenhanced T1-weighted image (B), and hyperintense on T2-weighted image (C) and on single-shot echo-planar DW imaging using $b = 800\ s/mm^2$ (D). The lesion was assigned as category 4 or 3 by each observer with MDCT and non-contrast MRI. The lesion (arrows) showed progressive enhancement from on the pancreatic phase (E) to 3 min delayed phase (F) after administration of gadoxetic acid, indicating pancreatitis.

cyst sign on non-contrast MRI by both observers (Fig. 2). FP (including AIP) was less likely to show grade 3 hypointensity on T1WI because inflammatory cells and normal tissue are intermingled in FP [10], DWI and T2WI might be useful in that they complement T1WI in localizing the lesions [12,17]. In particular, when the signal of the tumor is obscured by obstructive pancreatitis on T1WI, DWI is beneficial to localize PDAC proximal to the obstructive pancreatitis [12]. Approximately 5–10% of Whipple procedures performed for suspected PDAC turn out to be benign disease on final surgical pathology [1–4].Therefore, the significantly higher NPV for non-contrast MRI compared to that of MDCT in this study has notable clinical value.

Among the significant MRI features for predicting PDAC, presence of peritumoral cyst had the highest odds ratio. Tanaka et al. [18] demonstrated that the presence of a pancreatic cyst has a hazard ratio of 3.1 for development of PDAC. According to another report, PDAC was seen even in regions remote from the pre-existing cystic lesion [19]. This phenomenon can be explained by the hypothesis that the same diffuse pathologic changes of the pancreas parenchyma lead to both cyst formation and cancer development. The peritumoral cyst sign may also be explained by the dilatation of a peritumoral side branch of the pancreatic duct, since most PDACs originate from the ductal cells, infiltrate adjacent structures, and accompany desmoplasia. In addition, according to a previous report, a single small retention cyst (0.5–1.5 cm) was sometimes found at the periphery of PDACs [20]. Kim et al. [21] found that perilesional cyst on MDCT was more often seen in PDAC demonstrating only p-duct dilatation without a visible mass in comparison to benign lesions that cause p-duct dilatation (36.4% vs. 10.5%). However, MDCT might be limited in delineating small pancreatic cysts or minute p-duct changes given its low contrast resolution and/or coexisting fatty infiltration. Indeed, we found that 84.5% of PDAC were accompanied by tiny peritumoral cysts on T2WI. We believe that most of these cysts represent dilated side branches of the pancreatic duct, even though it was difficult to determine the location of some tiny cysts as to whether they were peritumoral or intratumoral. In

this study, the ductal cut-off sign had the second highest odds ratio, which was partly in agreement with a previous report [7]. The apparent hypointensity of the lesion revealed on T1WI, along with the recognition of p-duct cut off and peritumoural tiny cyst on T2WI, made it possible to correctly classify 33 and 29 indeterminate lesions as PDAC on MDCT by each observer, respectively.

In a previous study, MDCT failed to detect 30% of small PDACs (≤ 20 mm) using standardized CT protocol for the pancreas obtained within 18 months before histopathologic diagnoses [22]. Meanwhile, endoscopic ultrasound (EUS) and MRI are considered the most accurate techniques for pancreatic imaging for screening purpose as MRI is very sensitive for the detection of even the smallest cysts and EUS seems to be the most sensitive for the early detection of small solid lesions [23,24]. In our study, all PDACs were detected on at least one MRI sequence (including T1WI, T2WI, and DWI). T2WI is useful for detecting the morphology of ductal change and peritumoral cysts, and therefore identifying a lesion as PDAC. Therefore, we speculated that non-contrast MRI could serve as a good screening tool for PDAC while contrast-enhanced imaging may be considered as an additional tool for tumor staging.

Our study has several limitations. The study is subject to selection bias because we retrospectively selected the study population. The binary distinction between PDAC and FP might have artificially simplified the clinical scenario. However, other types of pancreatic tumors have their own unique characteristics that are distinguishable from FP. In addition, we were not able to precisely correlate the imaging findings and histological findings because this was a retrospective study in which pathological analysis was based on pathology reports. Therefore, in some cases, it was difficult to pinpoint the exact location of small cysts whether they are intratumoral or peritumoral. Another limitation is that pancreatic MRI in our institution was obtained using gadoxetic acid for enhanced detection of liver lesions [25]. Although prior studies showed similar enhancement features of PDAC and AIP using MRI with conventional gadolinium agents [8,26], we are uncertain whether our results apply to MRI using conventional gadolinium agents.

In conclusion, non-contrast MRI outperformed MDCT in the diagnosis of PDAC and its differentiation from FP with regard to accuracy, sensitivity, and NPV. The diagnostic performance of non-contrast MRI was similar to that of combined non-contrast and gadoxetic acid–-enhanced MRI. Therefore, non-contrast MRI could be a useful alternative to combined non-contrast and gadoxetic acid–enhanced MRI in the diagnosis of PDAC.

Funding

This research did not receive any specific grant from funding agencies in the public, commercial, or not-for-profit sectors.

References

[1] Adsay NV, Basturk O, Klimstra DS, Klöppel G. Pancreatic pseudotumors: non-neoplastic solid lesions of the pancreas that clinically mimic pancreas cancer. Semin Diagn Pathol 2004;21:260–7.
[2] Okun SD, Lewin DN. Non-neoplastic pancreatic lesions that may mimic malignancy. Semin Diagn Pathol 2016;33:31–42.
[3] Ho CK, Kleeff J, Friess H, Buchler MW. Complications of pancreatic surgery. HPB (Oxford) 2005;7:99–108.
[4] Zamboni G, Capelli P, Scarpa A, et al. Nonneoplastic mimickers of pancreatic neoplasms. Arch Pathol Lab Med 2009;133:439–53.
[5] Blouhos K, Boulas KA, Tsalis K, Hatzigeorgiadis A. The isoattenuating pancreatic adenocarcinoma: review of the literature and critical analysis. Surg Oncol 2015;24:322–8.
[6] Kim M, Jang KM, Kim JH, et al. Differentiation of mass-forming focal pancreatitis from pancreatic ductal adenocarcinoma: value of characterizing dynamic enhancement patterns on contrast-enhanced MR images by adding signal intensity color mapping. Eur Radiol 2017;27:1722–32.
[7] Choi SY, Kim SH, Kang TW, Song KD, Park HJ, Choi YH. Differentiating mass-forming autoimmune pancreatitis from pancreatic ductal adenocarcinoma on the basis of contrast-enhanced MRI and DWI findings. AJR Am J Roentgenol 2016;206:291–300.
[8] Hur BY, Lee JM, Lee JE, et al. Magnetic resonance imaging findings of the mass-forming type of autoimmune pancreatitis: comparison with pancreatic adenocarcinoma. J Magn Reson Imaging 2012;36:188–97.
[9] Sugiyama Y, Fujinaga Y, Kadoya M, et al. Characteristic magnetic resonance features of focal autoimmune pancreatitis useful for differentiation from pancreatic cancer. Jpn J Radiol 2012;30:296–309.
[10] Kim HJ, Kim YK, Jeong WK, Lee WJ, Choi D. Pancreatic duct "icicle sign" on MRI for distinguishing autoimmune pancreatitis from pancreatic ductal adenocarcinoma in the proximal pancreas. Eur Radiol 2015;25:1551–60.
[11] Kim JH, Park SH, Yu ES, et al. Visually Isoattenuating pancreatic adenocarcinoma at dynamic-enhanced CT: frequency, clinical and pathologic characteristics, and diagnosis at imaging examinations. Radiology 2010;257:87–96.
[12] Park MJ, Kim YK, S-y Choi, Rhim H, Lee WJ, Choi D. Preoperative detection of small pancreatic carcinoma: value of adding diffusion-weighted imaging to conventional MR imaging for improving confidence level. Radiology 2014;273:433–43.
[13] Kanda T, Fukusato T, Matsuda M, et al. Gadolinium-based contrast agent accumulates in the brain even in subjects without severe renal dysfunction: evaluation of autopsy brain specimens with inductively coupled plasma mass spectroscopy. Radiology. 2015;276:228–32.
[14] Bodily KD, Takahashi N, Fletcher JG, et al. Autoimmune pancreatitis: pancreatic and extrapancreatic imaging findings. AJR Am J Roentgenol 2009;192:431–7.
[15] Yang DH, Kim KW, Kim TK, et al. Autoimmune pancreatitis: radiologic findings in 20 patients. Abdom Imaging 2006;31:94–102.
[16] Wakabayashi T, Kawaura Y, Satomura Y, et al. Clinical and imaging features of autoimmune pancreatitis with focal pancreatic swelling or mass formation: comparison with so-called tumor-forming pancreatitis and pancreatic carcinoma. Am J Gastroenterol 2003;98:2679–87.
[17] Jang KM, Kim SH, Kim YK, Song KD, Lee SJ, Choi D. Missed pancreatic ductal adenocarcinoma: assessment of early imaging findings on prediagnostic magnetic resonance imaging. Eur J Radiol 2015;84:1473–9.
[18] Tanaka S, Nakao M, Ioka T, et al. Slight dilatation of the main pancreatic duct and presence of pancreatic cysts as predictive signs of pancreatic cancer: a prospective study. Radiology 2010;254:965–72.
[19] Tada M, Kawabe T, Arizumi M, et al. Pancreatic cancer in patients with pancreatic cystic lesions: a prospective study in 197 patients. Clin Gastroenterol Hepatol 2006;4:1265–70.
[20] Kosmahl M, Pauser U, Anlauf M, Kloppel G. Pancreatic ductal adenocarcinomas with cystic features: neither rare nor uniform. Mod Pathol 2005;18:1157–64.
[21] Kim SW, Kim SH, Lee DH, et al. Isolated Main pancreatic duct dilatation: CT differentiation between benign and malignant causes. AJR Am J Roentgenol 2017;209:1046–55.
[22] Yoon SH, Lee JM, Cho JY, et al. Small (< /= 20 mm) pancreatic adenocarcinomas: analysis of enhancement patterns and secondary signs with multiphasic multidetector CT. Radiology 2011;259:442–52.
[23] Krishna SG, Rao BB, Ugbarugba E, et al. Diagnostic performance of endoscopic ultrasound for detection of pancreatic malignancy following an indeterminate multidetector CT scan: a systemic review and meta-analysis. Surg Endosc 2017;31:4558–67.
[24] Harinck F, Konings IC, Kluijt I, et al. A multicentre comparative prospective blinded analysis of EUS and MRI for screening of pancreatic cancer in high-risk individuals. Gut 2016;65:1505–13.
[25] Motosugi U, Ichikawa T, Morisaka H, et al. Detection of pancreatic carcinoma and liver metastases with gadoxetic acid-enhanced MR imaging: comparison with contrast-enhanced multi-detector row CT. Radiology 2011;260:446–53.
[26] Muhi A, Ichikawa T, Motosugi U, et al. Mass-forming autoimmune pancreatitis and pancreatic carcinoma: differential diagnosis on the basis of computed tomography and magnetic resonance cholangiopancreatography, and diffusion-weighted imaging findings. J Magn Reson Imaging 2012;35:827–36.